Panoramas & Synthèses
38, 2012, p. 69–90

CUSPS IN INTERFACIAL PROBLEMS

by

Jens Eggers & Marco Antonio Fontelos

Abstract. — A wide range of equations related to free surface motion in two dimensions exhibit the formation of cusp singularities either in time, or as function of a parameter. We review a number of specific examples, relating in particular to fluid flow and to wave motion, and show that they exhibit one of two types of singularity: cusp or swallowtail. This results in a universal scaling form of the singularity, and permits a tentative classification.

***Résumé* (Problèmes interfaciaux et cusps).** — La formation de singularités en temps ou en fonction d'un paramètre est montrée pour un grand nombre d'équations liées au mouvement de surfaces libres. Nous examinons un certain nombre d'exemples spécifiques, en relation notamment avec l'écoulement d'un fluide et le mouvement des vagues. Nous montrons qu'ils présentent l'un des deux types de singularité : cusp ou queue d'aronde. Il en résulte un scaling universel qui permet de proposer une classification des singularités.

1. Introduction

In hydrodynamics, both viscous and inviscid free-surface flows have a natural tendency to "focus" into two-dimensional cusp [**14**] or three-dimensional tip singularities [**6**]. An example of such a singular surface deformation is seen in Fig. 1, right, which shows a jet of viscous fluid being poured into a container of the same liquid. The radius of curvature at the tip of the cusp becomes very small, but it remains finite, as we will see below.

As the speed of the jet increases, the cusp bifurcates into a new state, in which a thin sheet is entrained into the liquid, as illustrated in Fig. 2. Thus the formation of free-surface singularities is a natural pathway by which one phase is entrained into the other: the singularity serves as the "seed" for the entry of the other phase.

2000 *Mathematics Subject Classification.* — 35A20, 35R35, 58K35, 58Z05.
Key words and phrases. — Singularities, cusps, free surfaces, self-similarity.

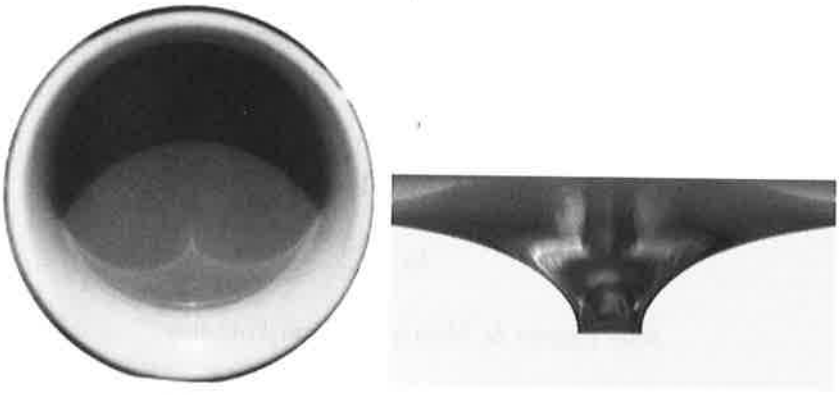

(a) (b)

FIGURE 1. Two examples of cusp singularities, observed in a very different context. On the left, a caustic in a coffee cup, which is a geometrical property of wave fronts. On the right a jet of viscous fluid is poured into bath, which deforms the free surface into a cusp singularity. In the cross section, imaged here, only one half of the cusp is seen.

Many such singularities occur in free-surface problems, a number of which we will discuss in the present paper. However our main focus is on the surprising similarities that exists between the structure of such singularities, although the underlying physics as well as their mathematical description may be quite different. This is illustrated in Fig. 1, which on the left, next to the viscous flow example, shows an image of a caustic in a coffee cup. The caustic, which is the locus of high light intensity, forms as a result of singularities of the wave front. As we will see below, the shape of the caustic (as well as of the wave front), has the same cusp singularity as the free surface cusp on the right, characterized by a scaling of the width of the cusp like $r^{3/2}$, where r is the distance from the apex. Singularities of wavefronts, *i.e.*, caustics, have been much studied [**18**], and their geometry can be classified using catastrophe theory [**2, 22**]. In the present review we point out that a similar classification appears to apply in a variety of nonlinear PDE problems, which describe the motion of a free (fluid) surface.

Let us begin by looking at possible singularities of curves from a purely geometrical perspective. The simplest case of self-intersection is that of the cusp, see Fig. 3. Let us assume that the coordinates x and y can be expanded into a Taylor series as function of some parameter, θ, and that we are interested in the neighborhood of $\theta = 0$. Since we describe phenomena up to arbitrary translations, the generic description is $x = a_1\theta$ and $y = a_2\theta$. However, by performing a rotation one can always make sure that one of the coefficients (a_2, say), is zero. The singular case corresponds to the situation where a_1 vanishes as well, so we put $x = \epsilon\theta$, with the singularity at $\epsilon = 0$.

Of course we are now required to expand to higher order. The next non-trivial order in y gives $y = \theta^2/2$, where the coefficient can be normalized by rescaling θ. The expansion in x has to be pursued to third order, otherwise the curve would be

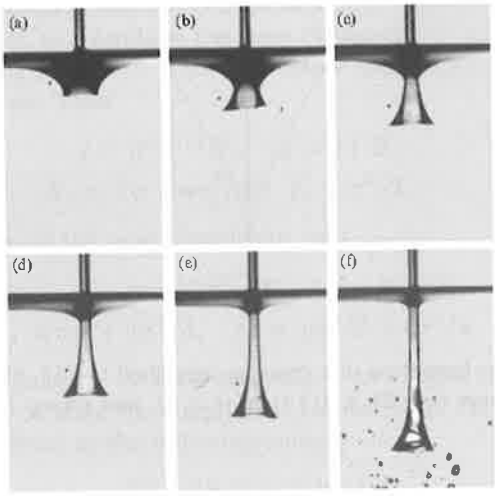

FIGURE 2. A jet of viscous liquid impinging on a bath of the same liquid, cf. [16]. Below a threshold velocity, the jet hollows the bath surface to a depth L, which increases with jet velocity up to a value of about 1cm (a). Above this threshold, air is entrained with the jet ((b) to (e)), and forms a stationary trumpet-like shape (f). At the same time, the surface of the bath around the jet relaxes to the shape of a static non-wetting meniscus, whose size is in the order of millimeters. The interval between two successive pictures is 130 ms. Note that the black line at the edge of the jet is no indication of the film thickness; it is due to the reflection of light by the curved air film of lower index of refraction.

degenerate for $\epsilon = 0$. Thus we finally have:

$$x = \epsilon\theta + a\theta^3/3, \quad y = \theta^2/2, \tag{1}$$

where a is an arbitrary constant. The quadratic coefficient in the expansion of x can be eliminated by a shift in θ, with subsequent rotation and translation. Thus up to translations and rotations, (1) is the only generic way the self-intersection of a curve in the plane can occur, as illustrated in Fig. 3. For $\epsilon < 0$ the curve self-intersects, at the critical point $\epsilon = 0$ a cusp is formed. It is clear from (1) that this cusp has the form $y = (x/a)^{2/3}$, *i.e.*, it is associated with a universal power law exponent. In catastrophe theory [2], (1) is the curve associated with the "cusp" catastrophe.

As we will see below, higher order singularities can also occur, which presumably is due to a hidden symmetry of the problem. As a result, the coefficient in front of the quadratic term vanishes at the same rate as the linear term in (1):

$$x = \epsilon\theta + a\theta^3/3, \quad y = \lambda\epsilon\theta^2/2 + b_1\theta^3/3 + b_2\theta^4/4. \tag{2}$$

For the curve described by (2) to be singular we must have $b_1 = 0$, otherwise $\epsilon = 0$ would simply correspond to a straight line. The coefficient λ can be eliminated by

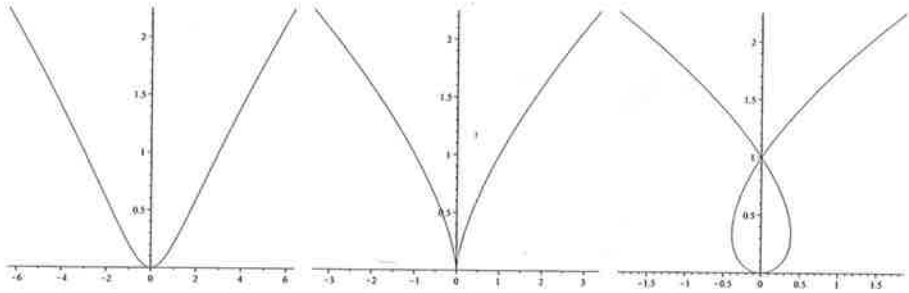

(a) (b) (c)

FIGURE 3. The formation of a cusp, as described by (1). Shown is a non-intersecting curve ($\epsilon = 2$), a 2/3 cusp ($\epsilon = 0$), and a loop ($\epsilon = -1$), from left to right.

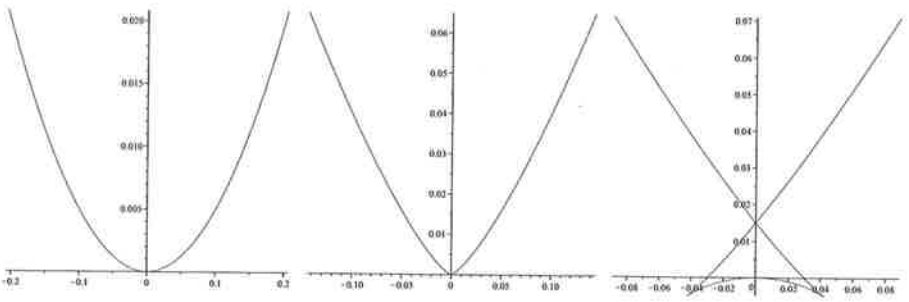

(a) (b) (c)

FIGURE 4. The formation of a swallowtail, as described by (4). Shown is a smooth minimum, ($\epsilon = 1$, left), a minimum with a 4/3 singularity ($\epsilon = 0$, right), and a swallowtail or double cusp ($\epsilon = -1/2$, right).

rescaling y and redefining b_2, so we arrive at the following generic form:

$$x = \epsilon\theta + a\theta^3/3, \quad y = \epsilon\theta^2/2 + b\theta^4/4, \tag{3}$$

which exhibits a much milder singularity. Here we have been assuming a symmetric bifurcation. This symmetry can be broken by a term linear in θ in the equation for y. For $\epsilon = 0$ the behavior is like $y \propto x^{4/3}$. For $\epsilon < 0$, the curve splits into two cusp singularities of the form shown in Fig. 3, where the case $b > a$ corresponds to $\epsilon > 0$ in the representation (1), $b < a$ to $\epsilon < 0$. In all the cases to be discussed below, we always find the particular case $a = b$, which means for $\epsilon < 0$ the solution is exactly at the cusp singularity. This is the swallowtail known from catastrophe theory, which can be seen as a collision of two cusps (see Fig. 4). It has the universal form

$$x = \epsilon\theta + a\theta^3/3, \quad y = \epsilon\theta^2/2 + a\theta^4/4, \tag{4}$$

once more with ϵ, a being parameters.

The two catastrophes (1) and (4) can occur either as function of time or of some control parameter. Let us introduce the time distance $t' = t_0 - t$ to the singularity, and assume the scaling $|\epsilon| = |t'|^\gamma$. The time before the singularity $t' > 0$ corresponds to $\epsilon > 0$, and *vice versa*. Then

$$x = |t'|^{3\gamma/2} X_c, \quad y = |t'|^\gamma Y_c, \tag{5}$$

$$X_c = \pm\sigma + a\sigma^3/3, \quad Y_c = \sigma^2/2, \tag{6}$$

is the self-similar form of the cusp singularity, and

$$x = |t'|^{3\gamma/2} X_s, \quad y = |t'|^{2\gamma} Y_s, \tag{7}$$

$$X_s = \pm\sigma + a\sigma^3/3, \quad Y_s = \pm\sigma^2/2 + a\sigma^4/4 \tag{8}$$

of the swallowtail singularity. In each case, the + or - signs correspond to the similarity function before or after the singularity, respectively. We remark that the cusp singularity can be written as the following cubic:

$$X_c^2 = 2Y_c(1 \pm 2aY_c/3)^2. \tag{9}$$

As we have mentioned before, the similarity function (7) valid *after* the singularity contains two cusp singularities, which occur for $\sigma = \pm 1/\sqrt{a}$. Thus if one writes $\sigma = \pm 1/\sqrt{a} + s$, shifts the cusp to the origin and performs a rotation, one obtains to leading order in s:

$$\begin{pmatrix} \pm as^3 \\ (a+1)s^2 \end{pmatrix} = \begin{pmatrix} 1 & \mp\sqrt{a} \\ \pm\sqrt{a} & 1 \end{pmatrix} \begin{pmatrix} X_s \pm 2/(3\sqrt{a}) \\ Y_s + 1/(4a) \end{pmatrix} \tag{10}$$

The + or - signs correspond the left and right cusp, respectively. This demonstrates that (X_s, Y_s) locally traces out a cusp after the swallowtail singularity, as seen in Fig. 4.

Table 1 summarizes the the problems to be studied in this paper, and cites the relevant sections. Each equation, to be discussed in more detail in the sections below, exhibits singularities which can be classified as either being of the "cusp" or the "swallowtail" type. Some are evolution equations, in which case we give the temporal

Equation	Type	γ	Section
Wave fronts	swallowtail	1	3
Hele-Shaw flow	cusp	1/2	4
Potential flow with free surface	swallowtail	//	5
Porous medium equation	cusp	//	6
Viscous flow with free surface	cusp	//	7
Born Infeld equation	swallowtail	1	8

TABLE 1. A summary of evolution equations discussed in this paper. The classification as "cusp" or "swallowtail" refers to (1) or (4), respectively. In the case of time-dependent problems, the exponent γ is defined by (5) or (7), depending on the type of singularity.

scaling exponent γ, others exhibit singularities as function of a parameter. In each case, we attempt to give physically motivated examples.

2. Complex mappings

We now look at the question of why any of the above singularities arise *dynamically*. The two-dimensional problems studied here can be written as a mapping of the physical domain to the unit disc, the free surface being represented as the circle. The appearance of a singularity is associated with this conformal map becoming non-invertible on the unit circle, as time or some other parameter reaches a critical value [4]. We show that a generic local structure of the conformal mapping corresponds exactly to the singularities identified above on geometrical grounds.

Let $z = f(\xi, t)$ be a complex mapping from the unit disk onto the physical domain, where t may be time or some other parameter. Let us assume that invertibility is lost at time t_0 for $\xi = \xi_0 = e^{\varphi_0 i}$. A local expansion yields

$$f(\xi,t) = a_0(t) + a_1(t)(\xi - e^{\varphi i}) + a_2(t)(\xi - e^{\varphi i})^2 + O((\xi - e^{\varphi i})^3), \tag{11}$$

where φ is a function of time, making use of the fact that we are allowed arbitrary time-dependent rotations in the ξ-plane. The more detailed functional form of φ will be chosen later, but we require it to be such that $\varphi(t) \to \varphi_0$ as $t \to t_0$. We are permitted arbitrary rotations in the physical plane z as well without altering the problem, so the image of f can be written as $ze^{i\delta}$, where δ is also an arbitrary time dependent function. We assume all functions of time to be continuous. Of course, their specific form will depend on the dynamics involved.

Let us introduce $\xi = e^{i\varphi}\zeta$ (mapping ξ_0 to 1), so that

$$ze^{i\delta} = a_0 + a_1 e^{i\varphi}(\zeta - 1) + a_2 e^{i2\varphi}(\zeta - 1)^2 + O((\zeta - 1)^3),$$

and thus the derivative yields

$$e^{i\delta}\frac{dz}{d\zeta} = a_1 e^{i\varphi} + 2a_2 e^{i2\varphi}(\zeta - 1) + O((\zeta - 1)^2). \tag{12}$$

The derivative (12) of the mapping is zero, signaling non-invertibility, if

$$\zeta = 1 - \frac{a_1 e^{-i\varphi}}{2a_2}, \tag{13}$$

which is a point outside the physical domain. We choose φ such that the second term $a_1 e^{-i\varphi}/a_2$ on the right hand side of (13) is real, which is consistent with $\varphi(t) \to \varphi_0$. Furthermore, we choose δ such that $a_1 e^{i(\varphi-\delta)}$ is real.

Now we shift the origin of the physical domain according to

$$\widetilde{z} = z - a_0 e^{-i\delta},$$

and introduce new expansion coefficients

$$\widetilde{a}_1 = a_1 e^{i(\varphi-\delta)}, \ \widetilde{a}_2 = a_2 e^{i(2\varphi-\delta)}.$$

The choices of δ and φ ensure that $\widetilde{a}_2$ and $\widetilde{a}_1$ are both real. This brings the local structure of the mapping to the standard form

$$\widetilde{z} = \widetilde{a}_1(\zeta - 1) + \widetilde{a}_2(\zeta - 1)^2 + O((\zeta - 1)^3). \tag{14}$$

The generic case for the boundary of the domain (which physically corresponds to the free surface) to become non-invertible is that $\widetilde{a}_1 \to 0$ as $t \to t_0$, while $\widetilde{a}_2$ remains bounded. In this simplest case (14) corresponds to a cusp. Namely, we parameterize the free surface by putting

$$\zeta = e^{i\theta}$$

and expand for small values of θ:

$$\begin{aligned}(\zeta - 1) &= \Big(-\frac{\theta^2}{2}\Big) + i\Big(\theta - \frac{\theta^3}{3!}\Big) + l.o.t.\\ (\zeta - 1)^2 &= -\theta^2 - \frac{\theta^3}{2}i + l.o.t.\\ (\zeta - 1)^3 &= -\theta^3 i + \frac{3}{2}\theta^4 + l.o.t.\end{aligned}$$

With x, y being the real and imaginary parts of $\widetilde{z}$, and remembering that a_1 is a small parameter of order θ^2, we find

$$x = -a_2\theta^2, \quad y = a_1\theta - a_2\theta^3/2,$$

which is the structure of the cusp (1).

The higher order case (3) is obtained if $\widetilde{a}_2$ also tends to zero, so that we have to expand further:

$$ze^{i\delta} = a_0 + a_1e^{i\varphi}(\zeta - 1) + a_2e^{i2\varphi}(\zeta - 1)^2 + a_3e^{i3\varphi}(\zeta - 1)^3 + O((\zeta - 1)^4).$$

Similar to the previous procedure, we choose φ and δ to make $\widetilde{a}_1 = a_1e^{i(\varphi-\delta)}$ and $\widetilde{a}_3 = a_3e^{i(3\varphi-\delta)}$ real, and define $\widetilde{a}_2 = a_2e^{i(2\varphi-\delta)} = a_{2R} + a_{2I}i$. Assuming that $\widetilde{a}_2$ is of the same order as $\widetilde{a}_1$, we can write at leading order

$$x = \Big(-\frac{\widetilde{a}_1}{2} - a_{2R}\Big)\theta^2 + \frac{3\widetilde{a}_3}{2}\theta^4, \quad y = \widetilde{a}_1\theta - \widetilde{a}_3\theta^3.$$

After re-parameterization $\theta \to -\frac{\theta}{2}$ and redefinition according to

$$\frac{a}{4} = \frac{3\widetilde{a}_3}{2^5}\ , \ \varepsilon = -\frac{\widetilde{a}_1}{2}\ , \ \frac{\lambda\varepsilon}{2} = \Big(-\frac{\widetilde{a}_1}{2} - a_{2R}\Big)$$

we arrive at

$$x = \frac{\lambda\varepsilon}{2}\theta^2 + \frac{a}{4}\theta^4, \quad y = \varepsilon\theta + \frac{b}{3}\theta^3. \tag{15}$$

For any finite λ, (15) is of the general form (3), up to a rescaling of x. In the special case $a = b$, and assuming $\lambda = 1$ without loss of generality, we obtain the swallowtail (4). If $\lambda = 0$, we obtain a $\frac{4}{3}$-singularity with a selfsimilar profile that is asymmetric near the origin.

3. The eikonal equation

3.1. Hamilton-Jacobi equation. — We consider the simplest case of wave propagation in a homogeneous medium, so the eikonal equation becomes $V_n = 1$: the normal velocity of the wave front is constant everywhere. We will only consider wave propagation in two dimensions, so the wave front is a curve. A straightforward way to solve the eikonal equation is to consider $y = h(x,t)$ so that one can write the equation in the form

$$\frac{\partial h}{\partial t} = \sqrt{1+h'^2}, \quad h(x,0) = h_0(x), \tag{16}$$

which expresses the condition of constant normal velocity. The prime denotes the derivative with respect to the spatial variable x.

To solve (16), we pass to the "particle" description; the equation for the wave front (16) is the Hamilton-Jacobi equation for the Hamiltonian

$$H(x,p) = -\sqrt{1+p^2}, \tag{17}$$

where $p = h_x$. The initial condition $(x_0, h_0'(x_0))$ yields a curve (x,p) in phase space, and the trajectories will be

$$\frac{dx}{dt} = \frac{\partial H}{\partial p} = -\frac{p}{\sqrt{1+p^2}}, \quad \frac{dp}{dt} = -\frac{\partial H}{\partial x} = 0. \tag{18}$$

Thus the solution to the particle problem is

$$p = \text{const} = h_0'(x_0), \quad x = x_0 - \frac{p}{\sqrt{1+p^2}}t = x_0 - \frac{h_0'(x_0)}{\sqrt{1+h_0'^2(x_0)}}t. \tag{19}$$

We can obtain an explicit solution by noting that

$$\frac{dh}{dx} = \frac{dh}{dx_0}\frac{dx_0}{dx} = h_0'(x_0),$$

where from (19)

$$\frac{dx}{dx_0} = 1 - \frac{h_0''}{\sqrt{1+h_0'^3}}t.$$

Integrating the resulting expression for dh/dx_0, we finally obtain

$$x = x_0 - \frac{h_0'}{\sqrt{1+h_0'^2}}t, \quad h = h_0(x_0) + \frac{t}{\sqrt{1+h_0'^2}}. \tag{20}$$

This is an explicit solution of (16), which has the additional advantage that it can be continued across any singularity the wave front may encounter.

A caustic is a place where rays meet, and thus $dx/dx_0 = 0$, $dy/dx_0 = 0$. The two conditions turn out to be equivalent, and one obtains

$$t_c = \frac{\sqrt{1+h_0'^2}^3}{h_0''} \equiv 1/\kappa. \tag{21}$$

It is also clear that points on the caustic correspond to singularities of the *wave front* [5]. The first singularity occurs at a time t_0 corresponding to the maximum of the

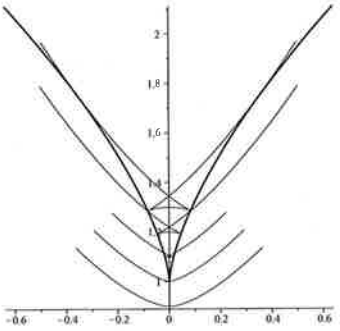

FIGURE 5. A caustic in a coffee cup. On the left, physical reality. On the right, the evolution of the wave front, as it passes through the swallowtail singularity. The caustic forms a 2/3-cusp, which corresponds to a swallowtail in terms of the shape of the wavefront.

curvature, for which there is optimal focusing. The universal structure is obtained by expanding h_0 in a series, which without loss of generality only contains even terms:

$$h_0 = a_1 x_0^2 + a_2 x_0^4 + \dots . \tag{22}$$

The first singularity occurs for $t_0 = 1/(2a_1) + \dots$, and an expansion leads precisely to (7), namely

$$\begin{aligned} x &= t'\sigma + a\sigma^3/3 \\ y &= 1/(2a_1) - t' + t'\sigma^2/2 + a\sigma^4/4, \end{aligned} \tag{23}$$

where $a = 3(a_1^3 - a_2)/(4a_1^4)$, and $\sigma = 2a_1 x_0$; the scaling exponent is $\gamma = 1$. After the singularity, $t' < 0$, (23) is a swallowtail, and the two cusp points trace out the caustic. This corresponds to the positions $\sigma_c = \pm\sqrt{-t'/a}$, and so to leading order the equation of the caustic is

$$x_c = \pm \frac{-4t'^{3/2}}{a^{1/2}}, \quad y_c = \frac{1}{2a_1} - t', \tag{24}$$

which is a normal 2/3-cusp, see Fig. 5.

3.2. conformal mapping. — There is a second way of solving the eikonal equation, closer to the methods to be used in the next sections, based in the use of a complex representation of the front. We present it here to stress the similarities between the different problems studied in this paper. If one identifies the points of the curve $(x(\sigma,t), y(\sigma,t))$ as points $z(\sigma,t) = x(\sigma,t) + iy(\sigma,t)$ in the complex plane, and the velocity $\mathbf{u} = (u,v)$ as the complex number $u + iv$, then

$$z_t = u + iv. \tag{25}$$

The tangent and normal vectors have a complex representation

$$\mathbf{t} = z_s, \quad \mathbf{n} = iz_s, \tag{26}$$

where s is the arclength parameter. Hence we can write

$$\mathbf{u}\cdot\mathbf{n} = \mathrm{Re}\,(iz_s\overline{z_t}) = -\mathrm{Im}(z_s\overline{z_t}),$$

and the eikonal equation is simply

$$\mathrm{Im}(z_s\overline{z_t}) = -1, \tag{27}$$

with the constraint $|z_s| = 1$. Equivalently, one can introduce an arbitrary parameter σ of the curve, and (27) becomes

$$\mathrm{Im}(z_\sigma\overline{z_t}) = -\frac{ds}{d\sigma}, \tag{28}$$

without the necessity of introducing a constraint.

We now demonstrate that (28) yields the same local solution as before, by verifying that (23) yields, at leading order, a solution of (28):

$$z_\sigma = (t' + a\sigma^2) + i(t'\sigma + a\sigma^3)\ ,\ z_t = -\sigma + i(1-\sigma^2/2)$$

$$\mathrm{Im}(z_\sigma\overline{z_t}) = -\Big(1+\frac{\sigma^2}{2}\Big)(t'+a\sigma^2)$$

$$\frac{ds}{d\sigma} = \sqrt{(t'+a\sigma^2)^2 + \sigma^2(t'+a\sigma^2)^2} = \Big(1+\frac{\sigma^2}{2}\Big)(t'+a\sigma^2+O(\sigma^4)).$$

4. Hele-Shaw flow

A Hele-Shaw cell consists of two closely spaced glass plates, partially filled with a viscous fluid. The problem is to find the time evolution of the free interface between fluid and gas. Here we consider the case that the fluid occupies a closed two-dimensional domain Ω. Within Ω, the pressure obeys $\Delta p = 0$, with boundary conditions

$$p = 0 \tag{29}$$

$$V_n = -\nabla p\cdot\mathbf{n} \tag{30}$$

on the free surface $\partial\Omega$. We write $z = x + yi$ and

$$p = \mathrm{Re}\Phi(\mathrm{z})$$

together with the conformal mapping

$$z = f(\xi,t), \quad \xi = re^{i\theta}, \tag{31}$$

which maps $|\xi| = 1$ onto $\partial\Omega$. If we consider

$$\Phi(z(\xi,t)) = \log\xi \quad \text{inside } \Omega,$$

then condition (29) is automatically satisfied. Moreover

$$-\nabla p\cdot\mathbf{n} = -\mathrm{Re}\Big(\frac{\partial\Phi}{\partial \mathrm{z}}\mathrm{iz_s}\Big) = -\mathrm{Re}\Big(\frac{\partial\Phi}{\partial\xi}\frac{1}{\mathrm{z}_\xi}\mathrm{iz_s}\Big) = -\mathrm{Re}\Big(\frac{1}{\xi\mathrm{z}_\xi}\mathrm{iz_s}\Big),$$

where s is the arclength parameter. Notice that one can write for $|\xi| = 1$, using $\xi = e^{i\theta(s,t)}$

$$z_s = z_\xi\xi_s = z_\xi\xi i\theta_s,$$

and hence

$$-\nabla p \cdot \mathbf{n} = \theta_s. \tag{32}$$

Since

$$V_n = \mathrm{Re}\,(\overline{z_t} i z_s) = -\theta_s \mathrm{Re}\,(\overline{z_t} \xi z_\xi)$$

we arrive, combining this with (32), at the equation

$$\mathrm{Re}\,(\overline{z_t} \xi z_\xi) = -1. \tag{33}$$

Noting that $\xi z_\xi = \frac{1}{i} z_\theta$, we finally obtain

$$\mathrm{Im}\,(z_\theta \overline{z_t}) = -1. \tag{34}$$

Equation (34) is identical to (27) except for the fact that the space variable is not the arclength parameter s, but the an arbitrary parameter θ. The non-invertibility of $f(\xi, t)$ signals the appearance of a singularity.

Now we will present an exact solution of (33), using a particular (polynomial) ansatz for the mapping 31 [**21, 20, 10, 13**]. We consider the simplest case of a quadratic:

$$f(\xi, t) = a_1(t)\xi + a_2(t)\xi^2, \tag{35}$$

and show that it leads to cusped solutions. However, we expect cusp formation to be a generic feature. The reason is that the formation of a singularity is associated to the non-invertibility of the conformal map $f(\xi, t)$ and this is equivalent to $f'(\xi, t)$ being zero at some point ξ_0 (at the time t_0 of formation of the singularity), which leads to a generic quadratic behavior of $f(\xi, t_0) = b_0 + b_2(\xi - \xi_0)^2$ near ξ_0. Other local expansions of $f(\xi, t_0)$ around ξ_0, of the form $f(\xi, t_0) = b_0 + b_n(\xi - \xi_0)^n$ with $n > 2$ are also possible. They would lead to different form of cusp, but cannot be generic since small perturbations of the initial data would produce quadratic terms.

Inserting (31),(35) into (34), we find a solution if the following system of ODEs is verified:

$$a_1 a_1' + 2a_2 a_2' = -1 \tag{36}$$

$$a_1 a_2' + 2a_2 a_1' = 0. \tag{37}$$

Direct integration of the equations leads to

$$\frac{1}{2} a_1^2 + \frac{B^2}{a_1^4} = A - t \tag{38}$$

$$A = \frac{1}{2} a_1^2(0) + a_2^2(0)\ ,\ B = a_2(0) a_1^2(0) \tag{39}$$

A singularity occurs when f fails to be invertible, that is

$$\frac{df}{d\xi} = a_1 + 2a_2\xi = 0 \Rightarrow \xi = -\frac{a_1}{2a_2} = -1 \tag{40}$$

or equivalently when

$$a_1 - 4\frac{B^2}{a_1^5} = 0 \Rightarrow a_1 = (2B)^{\frac{1}{3}}, a_2 = \frac{1}{2}(2B)^{\frac{1}{3}}. \tag{41}$$

From (38) one can compute the singularity time

$$t_0 = A - \frac{3}{4}(2B)^{\frac{2}{3}} = \frac{1}{2}a_1^2(0) + a_2^2(0) - \frac{3}{4}(2a_2(0)a_1^2(0))^{\frac{2}{3}}.$$

Now let us consider a particular solution, for instance

$$a_1(0) = 1\ ,\ a_2(0) = \frac{1}{16}, \tag{42}$$

so that

$$A = \frac{129}{256},\ B = \frac{1}{16},\ t_0 = \left(\frac{3}{4}\right)^4\ ,\ a_1(t_0) = \frac{1}{2},\ a_2(t_0) = \frac{1}{4}.$$

This implies the formation of a singularity at $x(\pi, t_0) = -\frac{1}{4}$ and $y(\pi, t_0) = 0$.

Local analysis leads to $a_1(t) = 1/2 + \widetilde{a}(t)$, where $3\widetilde{a}^2(t) \sim t_0 - t$. Thus the scale factor $\widetilde{a}(t)$ is

$$\widetilde{a}(t) \sim \frac{1}{\sqrt{3}}(t_0 - t)^{\frac{1}{2}} \equiv \frac{1}{\sqrt{3}}t'^{\frac{1}{2}}. \tag{43}$$

and $a_2(t) = 1/(16a_1^2(t)) \sim 1/4 - \widetilde{a}(t)$. Writing $\xi = -1 + \widetilde{\xi}$, we deduce

$$f(\xi, t) = a_1(t)\xi + a_2(t)\xi^2 \sim -1 - 2\widetilde{a}(t) + 3\widetilde{a}(t)\widetilde{\xi} + \frac{1}{4}\widetilde{\xi}^2. \tag{44}$$

Since

$$-1 + \widetilde{\xi} = -e^{i(\theta-\pi)} = -1 + (1 - e^{i\widetilde{\theta}}) \simeq -1 + \frac{\widetilde{\theta}^2}{2} - \frac{\widetilde{\theta}^4}{4!} - i\widetilde{\theta} + i\frac{\widetilde{\theta}^3}{3!} + O(\widetilde{\theta}^5)$$

one has

$$f(\xi, t) \sim -1 - 2\widetilde{a}(t) + 3\widetilde{a}(t)\Big(\frac{\widetilde{\theta}^2}{2} - \frac{\widetilde{\theta}^4}{4!} - i\widetilde{\theta} + i\frac{\widetilde{\theta}^3}{3!}\Big) - \frac{1}{4}\widetilde{\theta}^2 + \frac{1}{16}\widetilde{\theta}^4 - \frac{1}{4}\widetilde{\theta}^3 i + O(\widetilde{\theta}^5),$$

leading to the leading order contributions (all other terms are subdominant for small values of $\widetilde{a}(t)$ and $\widetilde{\theta}$):

$$x(\theta, t) + 1 \sim -2\widetilde{a}(t) - \frac{1}{4}\widetilde{\theta}^2 \tag{45}$$

$$y(\theta, t) \sim -3\widetilde{a}(t)\widetilde{\theta} - \frac{1}{4}\widetilde{\theta}^3, \tag{46}$$

which is the desired local solution we have been looking for.

Defining

$$X_c = -\frac{y}{6t'^{3/4}},\ Y_c = -\frac{x+1}{6t'^{1/2}} - \frac{1}{3\sqrt{3}},\ \Theta = \frac{\widetilde{\theta}}{2\sqrt{3}t'^{1/4}}, \tag{47}$$

one obtains the cusp (5), with $a = 9\sqrt{3}$ and the scaling exponent $\gamma = 1/2$. A different choice of initial conditions (42) will of course lead to a different value of the parameter a. In Figure 6 we represent the interface profiles corresponding to the example developed above at the initial time and at the time of formation of the cusp.

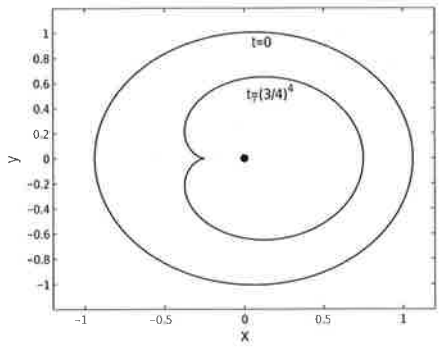

FIGURE 6. The formation of a cusp in Hele-Shaw problem with suction at the origin.

5. Potential flow

We consider the two-dimensional flow of an ideal fluid below a free surface. Inside the fluid, the fluid velocity $\mathbf{u} = (u, v)$ satisfies

$$\mathbf{u} = \nabla\phi, \quad \triangle\phi = 0, \tag{48}$$

where ϕ is the velocity potential. The free surface is convected by the fluid velocity, and the free surface is at constant pressure. We consider the simplest case of steady flow, as well as no body or surface tension forces. According to Bernoulli's equation, the fluid speed then has to be constant on the free surface.

Exact solutions to the flow problem can be found if the fluid domain is bounded by free surfaces and straight solid boundaries alone [**3**], by mapping the fluid domain onto the upper half of the complex plane, which we denote by ζ. Here, we consider only the even simpler case of only free boundaries, *i.e.*, that of a two-dimensional fluid drop. To this end, one introduces the complex potential $w = \phi + i\psi$, where ψ is the stream function. The derivative of w gives the fluid velocity:

$$\frac{dw}{dz} = u - iv \equiv qe^{-i\theta}, \tag{49}$$

where q is the particle speed.

On the fluid boundary, ψ is constant, and this constant can be chosen to vanish. Thus $w(\zeta)$ is real on the real axis (the boundary of the fluid drop), and so $dw/d\zeta$ must be real as well.

Following Hopkinson [**11**] we drive a fluid motion inside the drop by placing singularities inside the drop. We will consider the case of a vortex dipole and a vortex at the same point. We have

$$\frac{dw}{d\zeta} = \frac{dw}{dz}\frac{dz}{d\zeta}, \tag{50}$$

where $dz/d\zeta$ contains no singularities in the upper ζ plane, since the representation of the fluid flow must be conformal. But this means that $dw/d\zeta$ must have the

same singularities as dw/dz, except that we now have the freedom to choose the position of the two singularities and the orientation of the vortex doublet arbitrarily. Thus if we choose the two singularities at $\zeta = i$, and the orientation of the doublet toward the positive real axis, the potential for the doublet must locally look like $w \propto 1/(\zeta - i) - im \ln(\zeta - i)$. Here m is the relative strength of the vortex.

To insure that $dw/d\zeta$ also obeys the boundary condition, one has to add image singularities at $\zeta = -i$:

$$\frac{dw}{d\zeta} = \frac{1}{(\zeta - i)^2} + \frac{1}{(\zeta + i)^2} - im\Big(\frac{1}{\zeta - i} - \frac{1}{\zeta + i}\Big). \tag{51}$$

Depending on the value of m, two different cases arise. For simplicity, we only consider the case $m < 1$, in which

$$\frac{dw}{d\zeta} = \frac{2(1+m)(\zeta^2 - \gamma^2)}{(\zeta^2 + 1)^2}, \tag{52}$$

Where $\gamma = \sqrt{(1-m)/(1+m)}$ real.

Manifestly, $dw/d\zeta$ is real on the real axis, and has the right singularities at $\zeta = i$. However, the information contained in (51) is not enough to reconstruct the mapping $z(\zeta)$ we are after. Following Kirchhoff [**15**] and Planck [**19**], we define another function

$$\Omega = \ln \frac{dz}{dw} \equiv -\ln q + i\theta, \tag{53}$$

which will also be represented in the ζ-plane. Since q is constant along the free surface, and choosing units such that $q = 1$, the function Ω will be purely imaginary on the real ζ axis. To find Ω, we once more proceed in two steps.

First, we find the singularities of Ω. From the definition,

$$\Omega = -\ln \frac{dw}{d\zeta} + \ln \frac{dz}{d\zeta}, \tag{54}$$

where the second contribution is conformal in the upper half plane. This means Ω has singularities only for $\zeta = i$, where it behaves like $\Omega \propto 2\ln(\zeta - i)$. Second, we have to make sure that Ω is imaginary for real ζ, which is achieved by

$$\Omega = 2 \ln \frac{\zeta - i}{\zeta + i}. \tag{55}$$

Now we use the fact that

$$\frac{dz}{d\zeta} = \frac{dz}{dw}\frac{dw}{d\zeta} = e^{\Omega}\frac{dw}{d\zeta} = \frac{2(1+m)(\zeta^2 - \gamma^2)}{(\zeta + i)^4}. \tag{56}$$

This expression can be integrated to find the transformation $z(\zeta)$ between the fluid domain and the ζ-plane:

$$\frac{z}{2(1+m)} = -\frac{1}{\zeta + i} + \frac{i}{(\zeta + i)^2} + \frac{1 + \gamma^2}{3(\zeta + i)^3}. \tag{57}$$

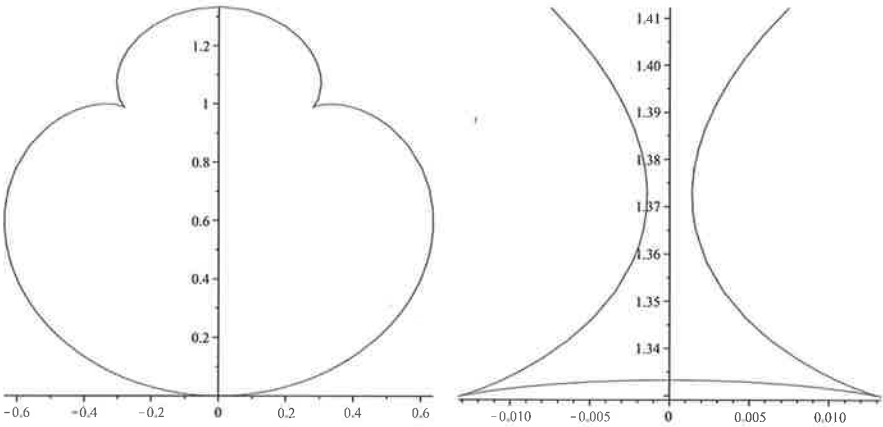

FIGURE 7. On the left, we show the entire drop for $m = 1/3$. On the right, a closeup of upper part of the drop for $m = 0.94$. The swallowtail has opened, and there is no more self-intersection.

From the real and imaginary part of this expression, we obtain

$$x = -(2(1+m))\zeta \frac{3\zeta^4 - (1+\gamma^2)\zeta^2 + 3\gamma^2}{3(\zeta^2+1)^3} \tag{58}$$

$$y = (2(1+m)) \frac{6\zeta^4 + 3(1-\gamma^2)\zeta^2 + 1 + \gamma^2}{3(\zeta^2+1)^3}. \tag{59}$$

The mapping is such that $\zeta = \pm\infty$ gets mapped to the origin. A typical drop shape, for $m = 1/3$, is shown in Fig. 7 (left); it exhibits two cusps. This feature is generic, in that it exists for a continuous range of values $0.9427 \geq m \geq 0$. On the right of show a closeup of the top of the drop, close to the upper end of his range.

The origin of the double cusp lies in a swallowtail transition for $m \approx 1$ that occurs at the point $x = 0$, $y = 4/3$ in real space. Namely, a local expansion of (59) gives with $m = 1 + \epsilon$

$$x = 2\epsilon\zeta + 4\zeta^3/3 \tag{60}$$

$$y = 4\epsilon\zeta^2 + 4\zeta^4, \tag{61}$$

where ζ is taken as real. The same expression results if the shape of the drop valid for $m > 1$ is expanded locally. The corresponding swallowtail is shown in Fig. 8 using the full solution Fig. 59. For m very close to the transition, the free surface must self-intersect, as shown in Fig. 8 (right). However, below a value of about $m \approx 0.9427$ the self-intersection disappears.

Another exact solution of potential flow that exhibits a cusp, but *in the presence of gravity* was found by Craya and Sautreaux [**7, 24, 8**]; liquid is layered above a two-dimensional ridge. At the crest of the ridge, which has opening angle $2\pi\gamma$, there

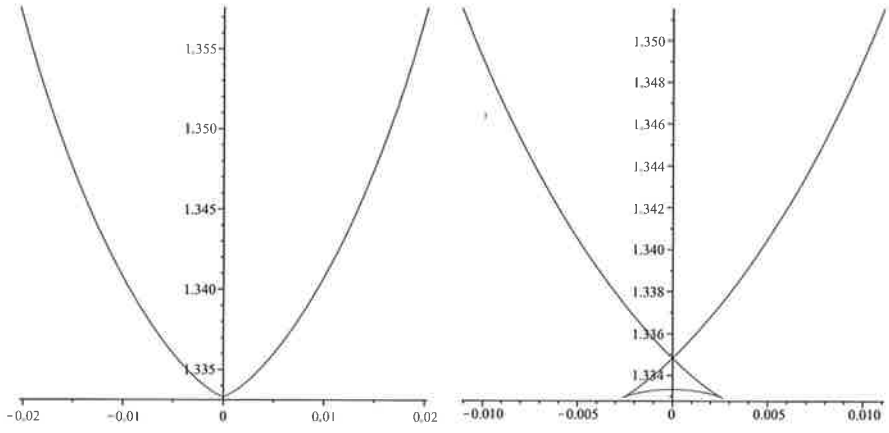

FIGURE 8. The birth of the swallowtail, as described by (59). For $m = 1$ (left) one is exactly at the transition, for $m = 0.98$ (right) one finds a swallowtail.

is a sink. For the special case $\gamma = 1/3$ there is an exact solution, given by

$$\frac{dz}{dl} = -i(2/3)^{1/3}\frac{1-l}{l^{1/3}(1+l)^{4/3}}, \tag{62}$$

where $l = \exp(-i\theta)$, $-\pi \leq \theta \leq \pi$. From a local analysis we find that

$$x = -\frac{3^{2/3}}{36}\theta^3, \quad y = -\frac{3^{2/3}}{12}\theta^2, \tag{63}$$

which is once more a 2/3 cusp. Of course this is to be expected, since gravity cannot change the local behavior near a cusp. However it is not clear where this comes from in terms of the swallowtail described above.

6. Porous medium equation

Another problem, closely related to the above, concerns the two-dimensional flow of oil in a porous medium. The oil is layered above heavier water, and is withdrawn through a sinkhole. The interface between the oil and the water is deformed, and forms a cusp at a critical flow rate. Inside the oil domain, one has to solve Laplace's equation for the velocity potential, cf. (48). In the stationary case, one has the usual condition of vanishing normal velocity on the free surface. However, from a pressure balance which includes the hydrostatic pressure, one obtains [**28, 29**]:

$$u^2 + v^2 = Kv, \tag{64}$$

where u, v are the horizontal and vertical components of the velocity, respectively.

Once more hodograph methods can be applied, but the problem can be solved only in the critical case at which there is cusp. Namely, in the subcritical case where there interface is smooth, $u = v = 0$ at the stagnation point below the sink. In the presence

of a singularity, $u = 0, v = K$ at the singularity, and the free surface gets mapped onto a circular arc in the hodograph plane. The resulting interface shape is

$$x = -\frac{2}{c\pi^2}\int_{-\beta}^{\sigma}\Big(\frac{\sqrt{a+1}}{\sigma_l} + \operatorname{arctanh}\sqrt{a+1}\Big)\Big(\frac{1}{a-\sigma_l} - \frac{1}{a-\sigma_s}\Big) \tag{65}$$

$$y = \frac{1}{c\pi}\Big(\ln\frac{\sigma_l - \sigma}{\sigma - \sigma_s} - \ln\frac{\sigma_l - 1 + \beta}{1 - \beta - \sigma_s}\Big), \tag{66}$$

where σ parameterizes the curve and σ_l and σ_s are determined from implicit equations involving c and β.

For $\beta = 1$ the curve defined by (65),(66) develops into a cusp. A local expansion yields

$$x = A\int_{-1}^{\sigma}\sqrt{1+a}\,da = \frac{2A}{3}(\sigma+1)^{3/2}, \tag{67}$$

where A is a constant. The y-coordinate is linear in $t+1$, thus (67) describes the usual 2/3 cusp. For $\beta < 1$ the interface self-intersects, at the line of symmetry, so this appears to be the generic cusp scenario. Numerical results confirm that the curve is smooth before the cusp forms (subcritical case), and a cusp forms in agreement with the exact solution (65),(66).

7. Viscous flow

Here the flow is governed by the Stokes equation, which in two dimensions can be written in terms of the stream function ψ, with $u = \psi_y$ and $v = -\psi_x$. The stream function obeys the biharmonic equation $\triangle^2\psi = 0$. In a stationary state, which we are considering, the surface of the fluid is a line with $\psi = \text{const}$. On this surface, we also have the surface stress condition

$$\sigma_{ij}n_j = \gamma\kappa n_i, \tag{68}$$

where γ is surface tension and κ the curvature of the interface. Once more the flow is driven by singularities, such as a vortex dipole [**14**].

A complex formulation of this problem was developed by Richardson [**23**]. The stream function is written as

$$\psi = \operatorname{Im}(f(z) + \overline{z}g(z)), \tag{69}$$

where f and g are analytic functions. The boundary conditions at the free surface can be shown to be

$$\operatorname{Im}\Big[\Big(\frac{\overline{dz}}{ds}\Big)f(z) + \overline{z}g(z)\Big] = \frac{\gamma}{4\eta}, \quad f(z) + \overline{z}g(z) = 0, \tag{70}$$

where η is the viscosity of the fluid.

In [**14**], the complex formulation (70) was used to calculate the following model problem: a vortex dipole of strength α is located at a distance d below a free surface of infinite extend. Surface tension is included in the description, but the effect of gravity

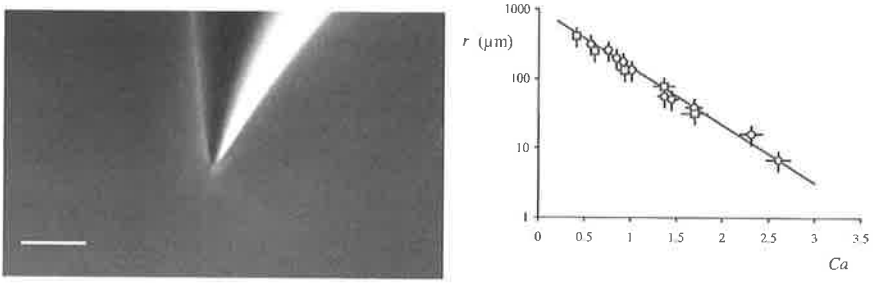

FIGURE 9. Experimental data on the cusping of a viscous fluid, taken from [**17**]. On the left, a closeup of the tip of a cusp on the surface of a viscous fluid; the scale bar corresponds to 200 μ m. On the right, the radius of curvature of the (almost) cusp as function of capillary number. In agreement with (80), the dependence is exponential.

is neglected. The deformation of the free surface by the viscous flow is determined by the capillary number

$$Ca = \frac{\alpha\eta}{d^2\gamma}, \tag{71}$$

which measures the ratio of viscous forces over surface tension forces. The solution of the problem is too involved to be presented here. The exact surface shape, in units of d, is given by the function

$$x = a\cos\theta + (a+1)\frac{\cos\theta}{1+\sin\theta}, \tag{72}$$

$$y = a(1+\sin\theta). \tag{73}$$

The parameter a is determined from the equation

$$4\pi Ca = \frac{-a(3a+2)^2K(m)}{1+a+\sqrt{-2a(a+1)}}, \tag{74}$$

where

$$m = \frac{2}{(-2a/(a+1))^{1/4} + ((a+1)/(-2a))^{1/4}} \tag{75}$$

and K is the complete elliptic integral of the first kind:

$$K(m) = \int_0^{\pi/2} \frac{d\theta}{\sqrt{1-m^2\sin^2\theta}}. \tag{76}$$

In (74) we have only reported the form of the equation for the more relevant case $Ca > 0$. Asymptotic analysis of (74)-(76) reveals that for large Ca,

$$a = -\frac{1}{3} + \epsilon, \quad \epsilon \approx \frac{32}{9}\exp\{-16\pi Ca\}. \tag{77}$$

It is easy to confirm that (72) yields a cusp for $a = -1/3$, *i.e.*, for $Ca = \infty$ or vanishing surface tension. If one expands around the cusp point by putting $\theta = \pi/2+\delta$, one obtains

$$x = -\frac{2\epsilon'}{3}\delta - \frac{\delta^3}{12} \tag{78}$$

$$y + \frac{2}{3} - 2\epsilon = \frac{\delta^2}{6}, \tag{79}$$

which is the generic cusp scenario (1). As is apparent from Fig. 3, the case $\epsilon < 0$ leads to self-intersection of the free surface, which is of course not physical. The radius of curvature of the cusp for $\epsilon > 0$ is given by

$$R \approx \frac{256}{3} \exp\{-32\pi Ca\}, \tag{80}$$

as found from (78),(77). The exponential dependence (80) has been confirmed experimentally (cf. Fig. 9).

8. Born-Infeld equation

The ideas presented here are not restricted to free surface problems. As an illustration we present a problem that appears in connection with string theory [**25**], but is also of long-standing interest in the theory of non-linear waves [**26**]. The Born-Infeld equation reads

$$z_{tt}(1 + z_x^2) - z_{xx}(1 - z_t^2) = 2z_x z_t z_{xt} \tag{81}$$

Hoppe [**12**] gave a general solution of the form

$$x'(t,\varphi) = \lambda \cos(f-g)\cos(f+g), \quad z'(t,\varphi) = \lambda \cos(f-g)\sin(f+g) \tag{82}$$

$$\dot{x}(t,\varphi) = -\sin(f-g)\sin(f+g), \quad \dot{z}(t,\varphi) = \sin(f-g)\cos(f+g), \tag{83}$$

where $f = f(\varphi + t/\lambda)$ and $g = g(\varphi - t/\lambda)$ are any two (smooth) functions and φ is a parameter. For (82) to be a graph, the tangent vector (82) should not be vertical, *i.e.*, we must require that $|f + g| < \pi/2$.

The curvature of this solution is

$$\kappa(t,\varphi) = \frac{f' + g'}{\cos(f-g)}, \tag{84}$$

so a singularity is expected whenever $f - g = \pi/2$. Let us assume for simplicity that $g(\zeta) = -f(-\zeta)$. I don't expect this to be a restriction on the class of possible singularities that can occur. Let $f(\zeta)$ have the local expansion

$$f(\zeta) = \pi/4 + a(\zeta - \zeta_0) - b(\zeta - \zeta_0)^2 + O(\zeta - \zeta_0)^3, \tag{85}$$

so together with the symmetry requirement we find

$$f - g = \pi/2 + 2a(t - \zeta_0) - 2b(\varphi^2 + (t - \zeta_0)^2). \tag{86}$$

The factor λ can be absorbed into a.

From this expression it is clear that ζ_0 has to be identified with the singular time t_0 and $a > 0$ for the solution to be regular for $t < t_0$. To expand around the singular

time, we put $t' = t_0 - t$. Similarly, one must have $b > 0$ (otherwise $f - g$ would be $\pi/2$ at an earlier time), and the singularity occurs at $\phi = 0$. Thus to leading order we have

$$f - g \approx \pi/2 - 2at' - 2b\varphi^2, \quad f + g \approx 2a\varphi, \tag{87}$$

from which we get

$$x' = 2at' + 2b\varphi^2, \quad z' = 4a^2t'\varphi + 4ab\varphi^3. \tag{88}$$

Integrating this expression, using the integrability condition (83), gives

$$x = t'\varphi + 2c\varphi^3/3, \quad z = t'\varphi^2/2 + c\varphi^4, \tag{89}$$

where we have used a rescaling of the parameter φ. This is of course exactly the swallowtail (4) with $\gamma = 1$.

9. Conclusions

We have presented several problems, mainly involving free surfaces or moving fronts, that exhibit the formation of cusps in finite time or as some parameter changes. We always find simple cusps with exponent 3/2 or the so-called swallowtail singularities, where a smooth curve develops a 4/3 singularity from which two simple cusps emerge. We have also shown that the local structure of the singularities is that of an algebraic curve (a cubic or a quartic) that evolves in a selfsimilar manner as time or some parameter varies, toward the formation of the singularity. The fact that 3/2 cusps develop is not accidental. It is closely linked to the nature of the physical problems under consideration, and the existence of mappings from a complex plane $\mathbb{C}$ to the $2D$ physical space identified with $\mathbb{C}$. We have shown that a family of such mappings parameterized with time or some other parameter can give rise to the formation of a singularity in the form of a cusp whenever the mapping becomes non-invertible. Generically, the holomorphic structure of the problem imposes that the singularity is exactly of the 3/2 type. Degenerate situations can lead to cusp singularities of a different type, the first degenerate singularity being a 4/3 cusp. A degenerate situation can become generic if, for example, the problem imposes an evolution with symmetries that forbid the 3/2 singularity.

It remains to be shown that other problems involving potential flows and the formation of singularities can also be cast in this framework. One of them is the evolution of vortex sheets, where a 3/2 singularity, called Moore's singularity, develops [**9**]. However, there is an important difference: a simple cusp has a local profile $y = \pm x^{3/2}$ with $x > 0$, (or $x = |y|^{2/3}$), while Moore's singularity is $y = |x|^{3/2}$ for all x. Singularities in vortex sheets are, therefore, not cusp singularities but of a weaker type that is only noticed in the curvature. Another example is the Rayleigh-Taylor instability in the context of ablation fronts, where a 5/4 singularity develops according to numerical simulations [**1**]. Thus again it is only the curvature that blows up, but the singularity is stronger than Moore's.

Of course, our results are confined to 2D geometries. A question that remains to be solved is whether these 3/2 or 4/3 singularities remain in 3D situations, even

with axial symmetry, or if one should expect a different type of generic cusp. We cannot rely on a holomorphic structure for the problem or the existence of conformal mappings. Perhaps generalizations of these notions, such as those in the context of Clifford algebras [**27**], could be as powerful as they are in 2D to explain generic forms of singularities. As far as we know, this has never been explored.

References

[1] C. Almarcha, P. Clavin, L. Duchemin & J. Sanz – "Ablative Rayleigh-Taylor instability with strong temperature dependence of the thermal conductivity", *J. Fluid Mech.* **579** (2007), p. 481–492.

[2] V. Arnol'd – *Catastrophe theory*, Springer-Verlag, Berlin, 1984.

[3] G. Batchelor – *An introduction to fluid dynamics*, Cambridge Mathematical Library, Cambridge University Press, Cambridge, 1999.

[4] M. Bazant & D. Crowdy – "Conformal mapping methods for interfacial dynamics", in *Handbook of Materials Modeling* (S. Yip, ed.), Springer, 2005, p. p. 1417.

[5] M. Berry – "Rays, wavefronts and phase: a picture book of cusps", in *Huygens' principle 1690–1990: theory and applications* (H. Blok, H. Ferweda & H. Kuiken, eds.), North-Holland Publishing Co., Amsterdam, 1992, p. 97–111.

[6] S. Courrech du Pont & J. Eggers – "Free-surface cusps associated with flow at low Reynolds numbers", *Phys. Rev. Lett.* **96** (2006), 034501.

[7] A. Craya – "Recherches théoriques sur l'écoulement de couches superposées de fluides de densités différentes", *La Houille Blanche* **4** (1949), no. 1, p. 44–55.

[8] C. Dun & G. Hocking – "Withdrawal of fluid through a line sink beneath a free surface above a sloping boundary", *J. Engrg. Math.* **29** (1995), no. 1, p. 1–10.

[9] J. Eggers & M. Fontelos – "The role of self-similarity in singularities of partial differential equations", *Nonlinearity* **22** (2009), no. 1, p. R1–R44.

[10] L. Galin – "Unsteady filtration with a free surface", *Dokl. Akad. Nauk. SSSR* **47** (1945), p. 246–249.

[11] B. Hopkinson – "On Discontinuous Fluid Motions involving Sources and Vortices", *Proc. London Math. Soc.* **S1-29**, no. 1, p. 142.

[12] J. Hoppe – "Conservation laws and formation of singularities in relativistic theories of extended objects", `http://arxiv:hep-th/9503069`, 1995.

[13] S. Howison – "Cusp development in Hele-Shaw flow with a free surface", *SIAM J. Appl. Math.* **46** (1986), no. 1, p. 20–26.

[14] J.-T. Jeong & H. Moffatt – "Free-surface cusps associated with flow at low Reynolds numbers", *J. Fluid Mech.* **241** (1992), p. 1–22.

[15] G. Kirchhoff – "Zur Theorie freier Flüssigkeitsstrahlen", *J. reine angew. Math.* **70** (1869), p. 289–298.

[16] E. Lorenceau, D. Quéré & J. Eggers – "Air Entrainment by a Viscous Jet Plunging into a Bath", *Phys. Rev. Lett.* **93** (2004), 254501.

[17] E. Lorenceau, F. Restagno & D. Quéré – "Fracture of a viscous liquid", *Phys. Rev. Lett.* **90** (2003), 184501.

[18] J. NYE – *Natural focusing and fine structure of light*, Institute of Physics Publishing, Bristol, 1999, Caustics and wave dislocations.

[19] M. PLANCK – "Zur theorie der flüssigkeitsstrahlen", *Wied. Ann.* **21** (1884), p. 499–509.

[20] P. POLUBARINOVA-KOCHINA – "Concerning unsteady motions in the theory of filtration", *Prikl. Matem. Mech.* **9** (1945), no. 1, p. 79–90.

[21] ———, "On the motion of the oil contour", *Dokl. Akad Nauk USSR* **47** (1945), p. 254–257.

[22] T. POSTON & I. STEWART – *Catastrophe theory and its applications*, Pitman, London, 1978.

[23] S. RICHARDSON – "Two-dimensional bubbles in slow viscous flows", *J. Fluid Mech.* **33** (1968), p. 475–493.

[24] C. SAUTREAUX – "Mouvement d'un liquide parfait soumis à la pesanteur. Détermination des lignes de courant", *J. Math. Pures Appl.* **7** (1901), p. 125–160.

[25] A. TSEYTLIN – "Born-Infeld action, supersymmetry and string theory", in *The many faces of the superworld*, World Sci. Publ., River Edge, NJ, 2000, p. 417–452.

[26] G. WHITHAM – *Linear and nonlinear waves*, John Wiley & Sons Inc., New York, 1974.

[27] S. WU – "Well-posedness in Sobolev spaces of the full water wave problem in 3-D", *J. Amer. Math. Soc.* **12** (1999), no. 2, p. 445–495.

[28] H. ZHANG & G. HOCKING – "Withdrawal of layered fluid through a line sink in a porous medium", *J. Austral. Math. Soc. Ser. B* **38** (1996), no. 2, p. 240–254.

[29] H. ZHANG, G. HOCKING & D. BARRY – "An analytical solution for critical withdrawal of layered fluid through a line sink in a porous medium", *J. Austral. Math. Soc. Ser. B* **39** (1997), no. 2, p. 271–279.

J. EGGERS, School of Mathematics, University of Bristol, University Walk, Bristol BS8 1TW, United Kingdom

M.A. FONTELOS, Instituto de Ciencias Matemáticas (ICMAT, CSIC-UAM-UCM-UC3M), C/ Serrano 123, 28006 Madrid, Spain